Inferring the Lifetime of Endosomal Protein Complexes by Fluorescence Recovery after Photobleaching

Veronika Gousseva,* May Simaan,† Stéphane A. Laporte,†‡ and Peter S. Swain*
*Centre for Non-Linear Dynamics, Department of Physiology; †Hormones and Cancer Research Unit, Department of Medicine; and ‡Department of Pharmacology & Therapeutics, McGill University, Montreal, Quebec, Canada

ABSTRACT Cellular signal transduction is dynamic, with signaling proteins continually associating and dissociating into and from protein complexes. Here we present a fluorescence recovery after photobleaching technique to determine the lifetime of protein complexes on intracellular vesicles. We use Bayesian inference based on a model that includes the diffusion of cytosolic proteins and their interaction with membrane-bound receptors. Our analysis is general: we incorporate prior information on protein diffusion, measurement error in determining fluorescence intensities, corrections for photobleaching, and variation in the concentration of receptors between vesicles. We apply our method to the complexes formed on endosomes by G-protein-coupled receptors and the protein β-arrestin. The lifetime of these complexes determines the recycling rate of the receptors. We find in mammalian cells that the bradykinin type 2 receptor and β-arrestin2 complex has a lifetime of $\sim$2 min, while the angiotensin II type 1A receptor and β-arrestin2 complex has a lifetime of $\sim$6 min. As well as allowing quantitative comparisons between experiments, our method provides in vivo parameters for systems biology simulations of signaling networks.

INTRODUCTION

With the invention of green fluorescent protein technologies, fluorescence recovery after photobleaching (FRAP) is becoming one of the methods of choice to investigate the dynamics of intracellular proteins (1–3). In a typical FRAP experiment, a region of the cell containing a fluorescently tagged protein is bleached and the recovery of the fluorescence in the bleached region is followed as fluorescent protein replaces bleached protein (4). The timescale of this recovery is partly set by diffusion (4), but can be significantly influenced by local geometry (5–7) and by the fluorescent protein interacting with other proteins (8–10).

Explicitly incorporating protein binding into models of fluorescence recovery has enabled protein binding affinities and rates to be estimated (11–14). Most of these studies have focused on nuclear phenomena. Here we apply FRAP to cytosolic signaling pathways and determine the lifetime of protein complexes. We specialize to endocytosed receptors and their interaction with cytosolic adaptor proteins, but our analysis is applicable to interactions occurring between any two proteins if one is predominantly cytosolic and the other is located on intracellular vesicles.

We apply our technique to G-protein-coupled receptors (GPCRs) and the adaptor protein β-arrestin. The addition of ligand to cells causes GPCRs to become activated and then desensitized. For many GPCRs, desensitization occurs after phosphorylation of the receptor by G-protein receptor kinases and the consequent binding of β-arrestin (15). Such binding uncouples the receptor from its G-proteins and targets the receptor for internalization by recruiting AP2 and clathrin (16,17). The strength of the β-arrestin and GPCR interaction determines the time that GPCRs are internalized: receptors that bind β-arrestin weakly recycle quickly to the plasma membrane, while receptors that bind β-arrestin strongly recycle slowly (18,19).

Our method infers the lifetime of the β-arrestin and GPCR complex from FRAP data, and therefore allows systematic investigation of how the β-arrestin and GPCR affinity is determined and regulated for different receptors. By using a fluorescently tagged β-arrestin, we are able to visualize endosomes that have β-arrestin and GPCR complexes in their membranes. If one of these endosomes is photobleached, its fluorescence slowly recovers as bleached arrestin dissociates from the receptors and is replaced by fluorescent, cytosolic arrestin. By recording how the fluorescence of a bleached endosome recovers, we gather data determined by the lifetime of the β-arrestin and GPCR complex (Fig. 1).

By estimating protein complex lifetimes, our method provides in vivo kinetic parameters. Such estimates are essential for accurate simulations of signaling networks, one of the goals of systems biology (20).

MATERIALS AND METHODS

Experimental protocol

Cell culture and transfection

Human embryonic kidney cells (HEK 293) were grown in Eagles minimal essential medium (Gibco, Grand Island, NY) supplemented with 10% (v/v) heat-inactivated fetal bovine serum (FBS; Gibco) and gentamicin (100 μg/ml; Gibco). Cells seeded in 35 mm glass-bottomed dishes were transfected using a conventional calcium phosphate coprecipitation method. Two and a half μg of DNA were mixed in a solution containing 125 mM $CaCl_2$ in HEPES-buffered saline (25 mM HEPES, pH 7.4, 140 mM NaCl, 0.75 mM

Submitted June 14, 2007, and accepted for publication August 13, 2007.

Address reprint requests to P. S. Swain, E-mail: swain@cnd.mcgill.ca; or S. A. Laporte, E-mail: stephane.laporte@mcgill.ca.

Editor: Enrico Gratton.

0006-3495/08/01/679/09 $2.00

doi: 10.1529/biophysj.107.115188

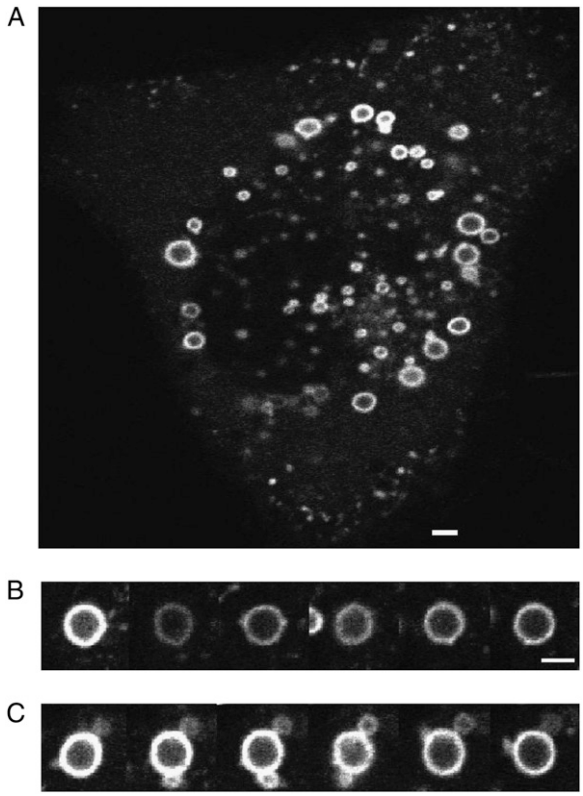

FIGURE 1 Confocal images of a HEK 293 cell and selected endosomes during a FRAP experiment. (*A*) A HEK 293 cell, expressing fluorescently tagged β-arrestin2, 15 min after exposure to bradykinin. Bradykinin receptors bound to fluorescent β-arrestin2 have been endocytosed making the endosomes visible. Scalebar 2 μm. (*B*) The bleached endosome. One endosome is deliberately photobleached and its recovery followed. The first image was taken before the endosome is bleached, and the others ~40, 60, 70, 120, and 150 s after bleaching. More typically, however, we take confocal images every 30 s. Scalebar 2 μm. (*C*) A control endosome, which is not deliberately bleached, but whose fluorescence intensity decreases by unavoidable photobleaching.

Na_2HPO_4) before being added to the cells. Plasmids encoding wild-type rat angiotensin II type 1A receptor, human bradykinin type 2 receptor, and β-arrestin2-T381-YFP are described elsewhere (19,21). β-arrestin2-YFP was obtained from Dr. M. G. Caron (Duke University, NC).

Photobleaching experiments

HEK 293 cells were transfected with bradykinin type 2 receptor and either β-arrestin2-YFP or β-arrestin2-381T-YFP (truncated β-arrestin2), or with β-arrestin2-YFP and the angiotensin II type 1A receptor. Forty-eight hours post-transfection, cells were treated with 1 μM of ligand (bradykinin or angiotensin II) for 15 min and then imaged live on a LSM-510 META laser-scanning confocal microscope (Zeiss, Jena, Germany) with a 60× oil immersion lens using a single line excitation at 514 nm and emission BP 530-600 nm filter sets. One endosome enclosed by a circle was bleached using the 514-nm laser line at full power (100 iterations), and the recovery of the yellow fluorescent protein (YFP) fluorescence was monitored over 3 min by scanning the whole cell at 30-s intervals. The cells were maintained at 37°C in minimal essential medium/20 mM HEPES on a heating stage (Harvard Apparatus, Holliston, MA) throughout the experiments. Quantification of the fluorescence intensities was calculated using MetaMorph software (Molecular Devices, Downingtown, PA).

Modeling

Solving for the recovery curve

In our experiment, β-arrestin exists in two forms: fluorescent (labeled with YFP) or nonfluorescent (either endogenous arrestin, which is not fluorescently labeled, or labeled arrestin that has become bleached). We assume that each endosome is spherical and that GPCRs are uniformly distributed over their surface (22). A typical experiment lasts for up to 5 min. We assume that this timescale is short enough that during the experiment no receptors enter or leave the endosome. The concentration of receptors at each endosome is therefore constant, but can be different from endosome to endosome. We experimentally confirmed this assumption by bleaching endosomes with fluorescently-tagged receptors. These endosomes never recovered in the time of our experiments. We also assume that the amount of fluorescent arrestin in the cell is conserved over the time of the experiment and is high enough that a bleached endosome will completely recover its original fluorescence intensity. We consider the recovery of the bleached endosome to be independent of the other endosomes. We adopt normal, isotropic, and homogeneous diffusion (diffusion with a constant diffusion coefficient) to describe movement of arrestin in the cytosol.

We consider only fluorescent arrestin because we assume that the interaction between arrestin and receptors at the endosome has reached equilibrium before the endosome is bleached. Bleaching does not affect the equilibrium between the total amount of receptor and the total amount of arrestin: it relabels the fluorescent arrestin on the endosome as nonfluorescent. Nonfluorescent arrestin can only affect the binding of fluorescent arrestin by altering the number of free receptors. If binding at the endosome has equilibrated before the bleach is applied, then the number of free receptors has, and remains at, its equilibrium value and the binding of fluorescent arrestin is independent of the binding of nonfluorescent arrestin (13).

We model the recovery of the bleached endosome as an ordinary differential equation coupled to a partial differential equation. Fluorescent arrestin at the endosome obeys

$$\frac{dC}{dt} = f^* A_S - bC, \tag{1}$$

where t is time; C is the concentration on the endosome of receptors bound by fluorescent arrestin; A_S is the concentration of cytosolic fluorescent arrestin at the surface of the endosome; b is the dissociation rate of an arrestin and receptor complex; and f^* is an effective association rate. It is the product of the actual association rate, f, and the equilibrium concentration of free receptors, R^{eq}: $f^* = fR^{eq}$. Assuming the endosome is completely bleached at the start of the experiment, Eq. 1 has initial condition $C(0) = 0$.

The concentration of cytosolic fluorescent arrestin, A, is a function of time, t, and distance, r, which is measured from the center of the bleached endosome. Initially, the free arrestin is at equilibrium: $A(r, t = 0) = A^{eq}$. Generally, $A(r, t)$ satisfies the spherically symmetric diffusion equation

$$\frac{\partial A}{\partial t} = \frac{D_A}{r^2}\frac{\partial}{\partial r}\left(r^2\frac{\partial A}{\partial r}\right), \tag{2}$$

where D_A is the diffusion coefficient of arrestin in the cytosol. We assume that the plasma membrane of the cell does not affect the recovery (we therefore set the plasma membrane to be far from the endosome) and impose a reflecting boundary condition there:

$$\left.\frac{\partial A}{\partial r}\right|_{r=\infty} = 0. \tag{3}$$

The second boundary condition is at the surface of the endosome. Each endosome has a different size and we denote the radius of the k^{th} bleached endosome as r_k. The total amount of fluorescent arrestin in the cell is conserved:

$$4\pi\int_{r_k}^{\infty} A(r,t)r^2 dr + 4\pi r_k^2 C(t) = \text{constant}. \tag{4}$$

Differentiating this conservation law with respect to time and using Eq. 2 to replace the time derivative of A gives

$$D_A \int_{r_k}^{\infty} dr \frac{\partial}{\partial r}\left(r^2 \frac{\partial A}{\partial r}\right) = -r_k^2 \frac{dC}{dt} \quad (5)$$

Integrating, and using Eq. 3, results in

$$D_A \left.\frac{\partial A}{\partial r}\right|_{r=r_k} = \frac{dC}{dt} \quad (6)$$

with Eq. 1 and with $A_S = A(r_k, t)$. If the concentration of the complex C increases, $dC/dt > 0$, then arrestin is depleted at the endosome and has a positive spatial gradient there. Similarly, if $dC/dt < 0$, arrestin is dissociating from receptors: the concentration of free arrestin at the endosome increases and there is a negative spatial gradient.

Eqs. 1, 2, 3, and 6 can be solved using Laplace transforms and numerically inverted (see Appendix). Along with C^{eq} and A^{eq}, this set of equations generates a recovery curve that is determined by three additional parameters: br_k^2/D_A, $f^* r_k/D_A$, and D_A/r_k^2. If diffusion is fast, i.e., if $br_k^2/D_A \ll 1$, an analytical solution is possible as

$$\frac{C(t)}{C^{eq}} = 1 + \left(\frac{C_i}{C^{eq}} - 1\right) e^{-b_{eff} t} \quad (7)$$

with $b_{eff} \simeq b$ (see Appendix). The initial value of C is C_i, which is zero if the endosome is fully bleached. The time of recovery is determined by one parameter: the dissociation rate of the receptor, b. Once a complex containing a bleached arrestin dissociates, diffusion is so rapid that the bleached arrestin immediately leaves the vicinity of the endosome and cannot rebind to a receptor.

Including photobleaching

Besides the deliberate photobleaching of the endosome at the beginning of the experiment, each fluorescent molecule may be permanently photobleached and become nonfluorescent every time an image is taken. We denote the probability of a fluorescent molecule surviving photobleaching when an image is taken as q, and so $1 - q$ of the fluorescent molecules are photobleached on average for each image. Although a binomial distribution with parameter q determines the number of fluorescent molecules that survive after an image is taken, we will ignore this variation and assume the survival of a constant fraction q of fluorescent molecules.

Consider reaction-limited binding with an initially fully bleached endosome and with images taken every Δt seconds. We predict that the fluorescence of the endosome at the j^{th} image, C_j, is related to the previous image, C_{j-1}, by

$$\frac{C_j}{C^{eq}} = q\left[1 + \left(\frac{C_{j-1}}{C^{eq}} - 1\right) e^{-b_{eff}\Delta t}\right], \quad (8)$$

from Eq. 7. The photobleaching terms form a geometric series, and so we find

$$\frac{C_j}{C_{eq}} = \frac{q(1 - e^{-b_{eff}\Delta t})(1 - q^j e^{-j b_{eff}\Delta t})}{1 - q e^{-b_{eff}\Delta t}}. \quad (9)$$

Equation 9, rather than Eq. 7, describes experimental data.

For the full solution of Eqs. 1 and 2, we numerically generate the recovery curve as a function of time. Assuming that the endosome is fully bleached, we start from zero fluorescence and move along the recovery curve a distance corresponding to a spacing Δt on the time axis. We bleach the value of the fluorescence we find by multiplying by q and then use linear interpolation to find the new bleached value of fluorescence on the recovery curve. Using this value as an initial condition, we repeat the procedure—moving along the recovery curve a spacing equivalent to Δt, bleaching, etc.—until fluorescence values have been generated for all the images.

The experimental data and measurement error

Each experiment gathers data from two to six endosomes and we typically fit data from ~10 experiments. In every experiment, one endosome is fully bleached, and images are taken of the recovery of this endosome and of the other, control, endosomes every 30 s for ~3 min. From the microscope images, we can estimate the size of each endosome by measuring its radius r_k.

We model two sources of variation in the data: first, we assume that each endosome has a different concentration of receptors and so a different concentration of receptors bound to fluorescent arrestin. We denote this concentration of fluorescent complex as C_k for endosome k and assume that the C_k are normally distributed with some mean C_0 and some standard deviation σ_C. Second, we assume that each fluorescent intensity has a measurement error, which we model as an additive correction to the true intensity. The additive correction is normally distributed with a mean of zero and a standard deviation of σ. A third source of variation is measurement error in the endosome radii. We ignore this variation, but it could be included.

Inferring the lifetime of the arrestin-receptor complex

The lifetime of the complex, τ_C, is related to the dissociation rate of the complex: $\tau_C = \log(2)/b$. From the data set, we will infer b, but because the product fR_k appears in Eq. 1 for endosome k, we can only infer values of fR_k from our data without prior information on the concentrations R_k. Consequently, we will learn little about the true association rate of the arrestin and receptor interaction, f, and therefore use the equilibrium relation

$$f_k^* = f R_k = \frac{bC_k}{A^{eq}} \quad (10)$$

to replace each f_k^*. The recovery is then a function of A^{eq}, the equilibrium cytosolic concentration of fluorescent arrestin, rather than f.

To infer b, we also infer the parameters determining the variation in the data—C_0, σ_C, and σ—and the bleaching parameter q. Each endosome has a different equilibrium concentration of free receptors, R_k. Rather than infer $\mathbf{R}$, a vector of the R_k for each endosome, we infer $\mathbf{C}$, a vector of the equilibrium concentrations of the fluorescent arrestin and receptor complex, because each C_k can be directly related to the data.

We use Bayesian inference (23). Bayesian inference interprets probability as a measure of our degree of belief. Our state of knowledge before an experiment is summarized as a prior probability distribution. Via Bayes's rule, we use the data from the experiment to update this prior probability to a posterior probability. For example, before an experiment our prior probability for the value of a parameter may simply be a uniform distribution over all positive values of the parameter. After we have gathered data, the corresponding posterior probability is a peaked distribution with the most probable value of the parameter being given by the peak and the width of the peak giving an estimate of the error in this most probable value.

We consider $P(b, A^{eq}, D_A, \mathbf{C}, C_0, \sigma_C, \sigma, q|\mathbf{D}^{(b)}, \mathbf{D}^{(c)})$ as our posterior probability. The data set consists of data from $M^{(b)}$ experiments: $\mathbf{D}^{(b)}$, the data for the $M^{(b)}$ bleached endosomes, and $\mathbf{D}^{(c)}$, the data for the $M^{(c)}$ control endosomes collected from all the experiments ($M^{(c)} > M^{(b)}$). We also have measurements of the radii of the endosomes, which we do not write explicitly. For each endosome, we measure its fluorescence intensity before the bleach and its fluorescence intensity for $N - 1$ consecutive images after the bleach. We therefore have N data points per endosome.

By Bayes's rule,

$$\begin{aligned} &P(b, A^{eq}, D_A, \mathbf{C}, C_0, \sigma_C, \sigma, q|\mathbf{D}^{(b)}, \mathbf{D}^{(c)}) \\ &\quad \sim P(\mathbf{D}^{(b)}, \mathbf{D}^{(c)}|b, A^{eq}, D_A, \mathbf{C}, C_0, \sigma_C, \sigma, q) \\ &\quad \times P(\mathbf{C}|C_0, \sigma_C) P(b) P(A^{eq}) P(D_A) P(C_0) P(\sigma_C) P(\sigma) P(q), \end{aligned} \quad (11)$$

where $P(b)$, $P(A^{eq})$, $P(D_A)$, $P(C_0)$, $P(\sigma_C)$, $P(\sigma)$, and $P(q)$ are all prior probabilities. We use the tilde (~) symbol to denote that terms independent

of the parameters of interest have been ignored. Such terms affect the normalization of the posterior probability. We assume that the recovery of the bleached endosome can only be affected by other endosomes through these endosomes acting as sources or sinks for fluorescent arrestin. We further assume that the quantity of cytosolic fluorescent arrestin is large enough for this effect to be negligible. Consequently, the data from the bleached and control endosomes are independent,

$$\begin{aligned}P(b,A^{\mathrm{eq}},D_{\mathrm{A}},\mathbf{C},C_0,\sigma_{\mathrm{C}},\sigma,q|\mathbf{D}^{(\mathrm{b})},\mathbf{D}^{(\mathrm{c})})\\ \sim P(\mathbf{D}^{(\mathrm{b})}|b,A^{\mathrm{eq}},D_{\mathrm{A}},\mathbf{C},\sigma,q)P(\mathbf{D}^{(\mathrm{c})}|\mathbf{C},\sigma,q)\\ \times P(\mathbf{C}|C_0,\sigma_{\mathrm{C}})P(b)P(A^{\mathrm{eq}})P(D_{\mathrm{A}})P(C_0)P(\sigma_{\mathrm{C}})P(\sigma)P(q),\end{aligned} \tag{12}$$

where we show only the relevant given variables. The data from each experiment are also independent,

$$P(\mathbf{D}^{(\mathrm{b})}|b,A^{\mathrm{eq}},D_{\mathrm{A}},\mathbf{C},\sigma,q)=\prod_{\mathrm{k}=1}^{\mathrm{M}^{(\mathrm{b})}}P(D_{\mathrm{k}}^{(\mathrm{b})}|b,A^{\mathrm{eq}},D_{\mathrm{A}},C_{\mathrm{k}},\sigma,q), \tag{13}$$

where $D_{\mathrm{k}}^{(\mathrm{b})}$ is the data for the k^{th} bleached endosome. We expand the probabilities $P(\mathbf{D}^{(\mathrm{c})}|\mathbf{C},\sigma,q)$ and $P(\mathbf{C}|C_0,\sigma_{\mathrm{C}})$ similarly.

We first consider the likelihood determined by the data for the bleached endosome. Let $a_{\mathrm{k}}=4\pi r_{\mathrm{k}}^2$ be the surface area of the k^{th} endosome and $d_{\mathrm{i,k}}^{(\mathrm{b})}$ be the i^{th} data point from the k^{th} bleached endosome. Modeling the measurement error as an additive correction from a normal distribution implies that (see below)

$$P(D_{\mathrm{k}}^{(\mathrm{b})}|b,A^{\mathrm{eq}},D_{\mathrm{A}},C_{\mathrm{k}},\sigma,q)\sim\sigma^{-\mathrm{N}}\exp\left[-\sum_{\mathrm{i}=0}^{\mathrm{N}-1}\frac{(d_{\mathrm{i,k}}^{(\mathrm{b})}-a_{\mathrm{k}}C_{\mathrm{k}}z_{\mathrm{i}}^{(\mathrm{k})})^2}{2\sigma^2}\right] \tag{14}$$

for the N fluorescence intensities, $d_{\mathrm{i,k}}^{(\mathrm{b})}$, measured for each bleached endosome. The predicted fluorescence intensities are derived from a rescaled version of the recovery curve, $\rho(t)$, found from solving Eqs. 1 and 2 (see Appendix). For endosome k,

$$z_{\mathrm{i}}^{(\mathrm{k})}=q\rho(\tau_{\mathrm{k}},\tilde{f}_{\mathrm{k}},\tilde{b}_{\mathrm{k}}|z_{\mathrm{i}-1}^{(\mathrm{k})}), \tag{15}$$

where τ_{k}, $\tilde{f}_{\mathrm{k}}$, and $\tilde{b}_{\mathrm{k}}$ are rescaled variables,

$$\tau_{\mathrm{k}}=\frac{D_{\mathrm{A}}\Delta t}{r_{\mathrm{k}}^2};\quad \tilde{f}_{\mathrm{k}}=\frac{r_{\mathrm{k}}C_{\mathrm{k}}b}{D_{\mathrm{A}}A^{\mathrm{eq}}};\quad \tilde{b}_{\mathrm{k}}=\frac{r_{\mathrm{k}}^2b}{D_{\mathrm{A}}}, \tag{16}$$

and where $\rho(\tau_{\mathrm{k}},\tilde{f}_{\mathrm{k}},\tilde{b}_{\mathrm{k}}|z_{\mathrm{i}-1}^{(\mathrm{k})})$ is the recovered fluorescence in dimensionless units after a rescaled time τ_{k} given that the dimensionless fluorescence was initially $z_{\mathrm{i}-1}^{(\mathrm{k})}$. Note that $\tilde{f}_{\mathrm{k}}$ is a function of A^{eq}. Photobleaching during each confocal scan is included by the factor q. The recovery curve ρ, which is normalized to have a completely recovered value of unity, has to be multiplied by the equilibrium fluorescence intensity of endosome k, $a_{\mathrm{k}}C_{\mathrm{k}}$, to be compared to the data. Here C_{k} is a concentration in fluorescence units per unit area and not an intensity. We define $z_0^{(\mathrm{k})}=1$ because $i=0$ refers to the image taken before the endosome was bleached and $z_0^{(\mathrm{k})}=0$ because the endosome is assumed to be bleached completely.

For the control endosomes, the additive normal model for the measurement noise implies

$$P(\mathbf{D}^{(\mathrm{c})}|\mathbf{C},\sigma,q)\sim\prod_{\mathrm{k}=1}^{\mathrm{M}^{(\mathrm{c})}}\sigma^{-\mathrm{N}}\exp\left[-\sum_{\mathrm{i}=0}^{\mathrm{N}-1}\frac{(d_{\mathrm{i,k}}^{(\mathrm{c})}-q^{\mathrm{i}}a_{\mathrm{k}}C_{\mathrm{k}})^2}{2\sigma^2}\right], \tag{17}$$

with the initial measurement, $d_{0,\mathrm{k}}^{(\mathrm{c})}$, having a predicted fluorescence intensity of $a_{\mathrm{k}}C_{\mathrm{k}}$ and each subsequent measurement being bleached by a factor q.

The equilibrium fluorescence concentrations of the endosomes are assumed to be normally distributed:

$$P(\mathbf{C}|C_0,\sigma_{\mathrm{C}})\sim\prod_{\mathrm{k}=1}^{\mathrm{M}^{(\mathrm{b})}+\mathrm{M}^{(\mathrm{c})}}\sigma_{\mathrm{C}}^{-1}\exp\left[-\frac{(C_{\mathrm{k}}-C_0)^2}{2\sigma_{\mathrm{C}}^2}\right]. \tag{18}$$

Consequently, Eq. 12 then implies

$$\begin{aligned}P(b,A^{\mathrm{eq}},D_{\mathrm{A}},\mathbf{C},C_0,\sigma_{\mathrm{C}},\sigma,q|\mathbf{D}^{(\mathrm{b})},\mathbf{D}^{(\mathrm{c})})\sim\sigma^{-\mathrm{N}(\mathrm{M}^{(\mathrm{b})}+\mathrm{M}^{(\mathrm{c})})}\sigma_{\mathrm{C}}^{-(\mathrm{M}^{(\mathrm{b})}+\mathrm{M}^{(\mathrm{c})})}\exp\left[-\sum_{\mathrm{k}=1}^{\mathrm{M}^{(\mathrm{b})}}\left\{\sum_{\mathrm{i}=0}^{\mathrm{N}-1}\frac{(d_{\mathrm{i,k}}^{(\mathrm{b})}-a_{\mathrm{k}}C_{\mathrm{k}}z_{\mathrm{i}}^{(\mathrm{k})})^2}{2\sigma^2}+\frac{(C_{\mathrm{k}}-C_0)^2}{2\sigma_{\mathrm{C}}^2}\right\}\right.\\ \left.-\sum_{\mathrm{k}=1}^{\mathrm{M}^{(\mathrm{c})}}\left\{\sum_{\mathrm{i}=0}^{\mathrm{N}-1}\frac{(d_{\mathrm{i,k}}^{(\mathrm{c})}-q^{\mathrm{i}}a_{\mathrm{k}}C_{\mathrm{k}})^2}{2\sigma^2}+\frac{(C_{\mathrm{k}}-C_0)^2}{2\sigma_{\mathrm{C}}^2}\right\}\right]P(b)P(A^{\mathrm{eq}})P(D_{\mathrm{A}})P(C_0)P(\sigma_{\mathrm{C}})P(\sigma)P(q),\end{aligned} \tag{19}$$

which is the posterior probability for b (and other parameters) given the entire FRAP data set.

Inferring the equilibrium fluorescence values for the bleached endosomes allows a better visual comparison between the data and the fitted recovery curves, but little information is gained by inferring values for the equilibrium fluorescence of the control endosomes. We therefore integrate out from Eq. 19 the C_{k} for the control endosomes and so reduce the number of $\mathbf{C}$ parameters by $M^{(\mathrm{c})}$. The exponent in Eq. 19 is quadratic in C_{k}. We integrate the C_{k} for the control endosomes from both sides of Eq. 19 by extending the range of integration to $-\infty$, which should contribute little error as the exponent will have a maximum at positive values of C_{k}. We find

$$\begin{aligned}P(b,A^{\mathrm{eq}},D_{\mathrm{A}},\mathbf{C},C_0,\sigma_{\mathrm{C}},\sigma,q|\mathbf{D}^{(\mathrm{b})},\mathbf{D}^{(\mathrm{c})})\sim\sigma^{-\mathrm{N}(\mathrm{M}^{(\mathrm{b})}+\mathrm{M}^{(\mathrm{c})})}\sigma_{\mathrm{C}}^{-(\mathrm{M}^{(\mathrm{b})}+\mathrm{M}^{(\mathrm{c})})}\exp\left[-\sum_{\mathrm{k}=1}^{\mathrm{M}^{(\mathrm{b})}}\left\{\sum_{\mathrm{i}=0}^{\mathrm{N}-1}\frac{(d_{\mathrm{i,k}}^{(\mathrm{b})}-a_{\mathrm{k}}C_{\mathrm{k}}z_{\mathrm{i}}^{(\mathrm{k})})^2}{2\sigma^2}+\frac{(C_{\mathrm{k}}-C_0)^2}{2\sigma_{\mathrm{C}}^2}\right\}\right]\\ \times\left(\prod_{\mathrm{k}=1}^{\mathrm{M}^{(\mathrm{c})}}\alpha_{\mathrm{k}}\right)^{-\frac{1}{2}}\exp\left[-\sum_{\mathrm{k}=1}^{\mathrm{M}^{(\mathrm{c})}}(\gamma_{\mathrm{k}}-\beta_{\mathrm{k}}^2/\alpha_{\mathrm{k}})\right]P(b)P(A^{\mathrm{eq}})P(D_{\mathrm{A}})P(C_0)P(\sigma_{\mathrm{C}})P(\sigma)P(q),\end{aligned} \tag{20}$$

where $\alpha_k = (1/2\sigma_C^2)+(a_k^2/2\sigma^2)\sum_{i=0}^{N-1} q^{2i}$ is the coefficient of C_k^2 in the second exponential term in Eq. 19, $\beta_k = (C_0/2\sigma_C^2)+(a_k/2\sigma^2)\sum_{i=0}^{N-1} d_{i,k}^{(c)} q^i$ is half the coefficient of C_k, and $\gamma_k = (C_0^2/2\sigma_C^2)+(1/2\sigma^2)\sum_{i=0}^{N-1}(d_{i,k}^{(c)})^2$ is the C_k independent term.

Equation 20, where $\mathbf{C}$ now refers only to the equilibrium fluorescence intensities of the bleached endosomes, is the posterior probability we use to infer b.

Numerical algorithm

Our strategy is to use a Metropolis-Hastings Markov chain Monte Carlo algorithm (24,25) to sample the parameters b, A^{eq}, D_A, $\mathbf{C}$, C_0, σ_C, σ, and q from the posterior probability (Eq. 20). We implement our algorithm in MATLAB (The MathWorks, Natick, MA), and our code is available on request. The efficiency of this algorithm is dependent on good initial estimates for the parameters.

Our approach is:

1. We find initial estimates for C_0, σ_C, σ, and q by considering only the data from the control endosomes, $\mathbf{D}^{(c)}$. We use maximum a posteriori estimates. The posterior probability $P(C_0, \sigma_C, \sigma, q|\mathbf{D}^c)$ is given by the term dependent on $\mathbf{D}^{(c)}$ in Eq. 20 (through β_k and γ_k) with the prior probabilities $P(C_0)$, $P(\sigma_C)$, $P(\sigma)$, and $P(q)$. We assume that these prior probabilities are uniformly distributed in a certain range and zero otherwise. The maximum likelihood and maximum a posteriori estimates for the parameters are then identical. We maximize $P(C_0, \sigma_C, \sigma, q|\mathbf{D}^c)$ using a simplex search method (fminsearch in MATLAB) to provide initial estimates of C_0, σ_C, σ, and q.
2. We find an initial estimate of b by using a Metropolis-Hastings method to fit the reaction-limited solution of the recovery curve, which depends only on b (Eq. 7). We set C_0, σ_C, σ, and q to the values that maximize $P(C_0, \sigma_C, \sigma, q|\mathbf{D}^c)$ and set the C_k to a normal sample with a standard deviation of σ_C around the initial measured fluorescence intensities of the endosomes. The Markov chain usually converges quickly because the recovery is only determined by one parameter.
3. We find initial estimates for A^{eq} and D_A and an improved estimate for b by maximizing the term dependent on the data from the bleached endosomes, $\mathbf{D}^{(b)}$, in Eq. 20 with respect to b, A^{eq}, and D_A. We use our first estimate of b as a lower bound for b. We set C_0, σ_C, σ, and q to the values that maximize $P(C_0, \sigma_C, \sigma, q|\mathbf{D}^c)$ and set the C_k again to a normal sample around the initial measured fluorescence intensities of the endosomes. We use a simplex search method (fminsearch in MATLAB).
4. We use a Metropolis-Hastings algorithm to sample from Eq. 20 using these initial estimates for b, A^{eq}, and D_A and for C_0, σ_C, σ, and q as starting values. We initially set the C_k to a normal sample from a distribution with mean C_0 and standard deviation σ_C. We set the step-size for b and A^{eq} by trial and error; D_A is sampled from a prior probability; we use the estimated errors in the initial fits of C_0, σ_C, σ, and q as their step-sizes (we estimate the errors by inverting the Hessian corresponding to the minimum of the negative logarithm of $P(C_0, \sigma_C, \sigma, q|\mathbf{D}^c)$); and the step-sizes for the C_k are all equal to the initial fitted value of σ_C.

The results of Fig. 4 are the mean of five different Monte Carlo runs.

Prior probability for D_A

One advantage of our Bayesian approach is that we can incorporate previous measurements of the diffusion rates of cytosolic proteins. The diffusion coefficient of green fluorescent protein (GFP) in the cytosol is $\sim 14\ \mu m^2\ s^{-1}$ (26,27). GFP has a mass of 27 kDa, whereas β-arrestin2 has a mass of 46 kDa. Assuming that the mass of a protein scales as its radius cubed, the measured diffusion coefficient of GFP and the Stokes-Einstein relation implies that the diffusion coefficient of the β-arrestin2 and YFP construct we use is $\sim 10\ \mu m^2\ s^{-1}$. We adopt the γ-distribution in the inset of Fig. 4 as the prior distribution of D_A. It has a broad peak at $\sim 10\ \mu m^2\ s^{-1}$ and is a distribution over only positive numbers.

For the simulations of Fig. 3, we use a prior probability for D_A that is constant in log-space: $P(D_A)dD_A = dD_A/D_A = d \log D_A$. Consequently, D_A is a priori equally likely to have any magnitude.

RESULTS

To confirm our algorithm, we first tested simulated data. We generated data using parameter values similar to those found from the experimental data at different signal/noise ratios and at different diffusion rates. We randomly set the size of each endosome, assigned each endosome an equilibrium concentration of fluorescent β-arrestin and receptor complex by sampling from a normal distribution, generated the corresponding recovery curves from Eqs. 1 and 2, bleached these curves by a factor q, and then added normally distributed measurement noise. Our simulated data look very similar to the measured data shown in Fig. 2.

To quantify the error in our inference, we use $|\log_2(b^{est}/b_0)|$ where b^{est} is the estimated value of b, the dissociation rate of the β-arrestin and receptor complex, and b_0 is the true value. For an exact estimate of b, the inference error will be zero; if b^{est} is twice or half b_0, the inference error is one. We define the signal/noise ratio to be the ratio of the estimated fluorescence intensity of the endosome before bleaching, $4\pi r_k^2 C_0$, to the estimated value of the measurement error, σ.

Our algorithm performs best in regimes where the recovery is reaction-limited (Fig. 3) or when the signal/noise ratio is high. If a typical reaction timescale, $1/b$, is greater than the diffusion timescale, r_k^2/D_A, where r_k is the radius of an endosome and D_A is the diffusion coefficient of cytosolic arrestin, then the recovery is reaction-limited and is principally set by b (see Appendix). In this regime, because of the simplicity of the recovery curve, our algorithm performs well with the inference error always <0.15, and the maximum inference error corresponding to an over- or under-estimation of b of only 8% (Fig. 3 *A*). If the recovery is closer to diffusion-limited, $r_k^2 b/D_A \gg 1$, then b, D_A, and A^{eq}, the equilibrium concentration of cytosolic β-arrestin, all determine the recovery. For high signal/noise ratios our algorithm still performs well, but when the signal/noise ratio decreases to 10, the inferred values of b are over- or underestimated by $>500\%$ and are incorrect by an order of magnitude (Fig. 3 *B*). The data is too noisy to fit the three parameters determining the recovery curve. Deep in the diffusion-limited regime, the reaction between β-arrestin and the receptor is at quasi-equilibrium throughout the recovery (see Appendix), and it is impossible to recover the lifetime of the complex without additional information.

We expect that the recovery will be reaction-limited for many signaling proteins. In our simulations, our algorithm only begins to fail when the diffusion coefficient for cytosolic arrestin is very low, $D_A = 0.001\ \mu m^2\ s^{-1}$. The diffusion coefficient for cytosolic GFP is $\sim 14\ \mu m^2\ s^{-1}$ (26,27). Assuming the radius of an endosome is $\sim 1\ \mu m$, a diffusion coefficient of this magnitude implies that b must be $>14\ s^{-1}$, or the lifetime of the protein complex must be <0.05 s, for

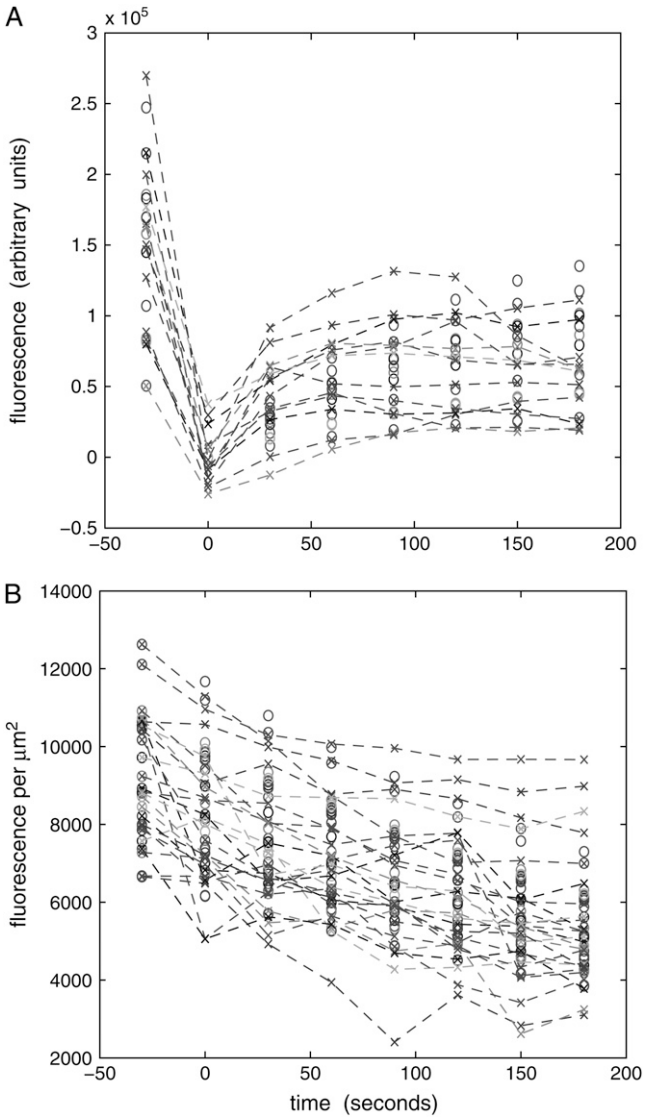

FIGURE 2 Fluorescence data for β-arrestin2 and the bradykinin type-2 receptor from 13 different FRAP experiments. (*A*) Fluorescence intensities for the bleached endosomes, including the image before bleaching, just after bleaching, and six subsequent images. Bleaching occurs at time 0, and the data are normalized across the experiments to have a mean fluorescence of zero at the bleach. Data points are marked by crosses and are joined by dashed lines to guide the eye. (*B*) Data from 26 control endosomes showing the effects of photobleaching during each confocal scan. Even though we plot the fluorescence concentration (the fluorescence intensity divided by the surface area of the endosome assuming each endosome is spherical), there is still a significant spread in the data. In both plots, circles are predicted values using the inferred parameters found by our algorithm.

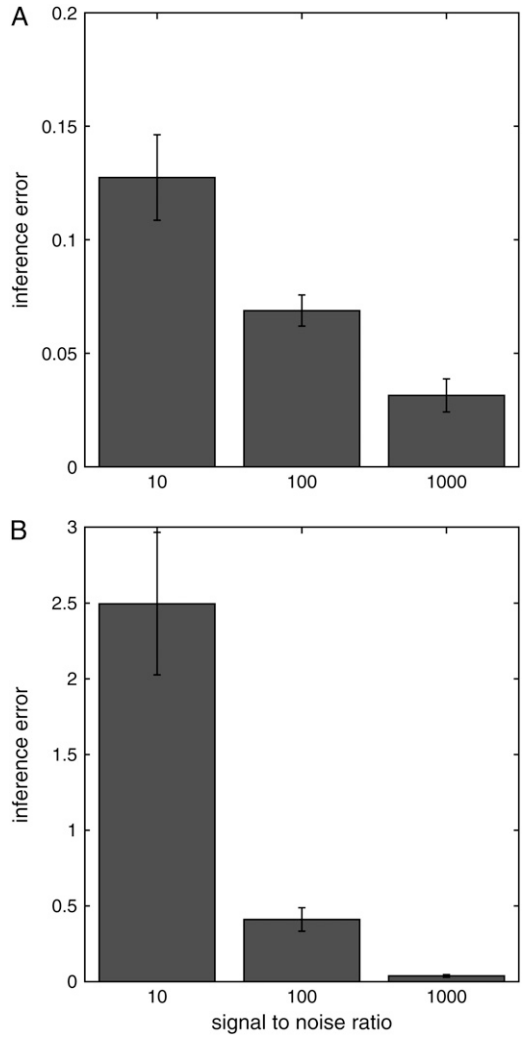

FIGURE 3 Evaluation of the inference algorithm for simulated data. The inference error is $|\log_2(b^{\mathrm{est}}/b_0)|$, where b^{est} is the estimated value of b and b_0 is the true value. We fit data with different signal/noise ratios where we define the signal/noise ratio as $4\pi r_{\mathrm{k}}^2 C_0/\sigma$. (*A*) The reaction and diffusion timescales are similar: $b_0 r_{\mathrm{k}}^2/D_{\mathrm{A}} \simeq 0.6$ ($D_{\mathrm{A}} = 0.1\ \mu\mathrm{m}^2\ \mathrm{s}^{-1}$); (*B*) the reaction timescale is faster than the diffusion timescale: $b_0 r_{\mathrm{k}}^2/D_{\mathrm{A}} \simeq 60$ ($D_{\mathrm{A}} = 0.001\ \mu\mathrm{m}^2\ \mathrm{s}^{-1}$). Note the different scales on the *y* axis. The parameter values used to generate the data were $C_0 = 0.9, \sigma_{\mathrm{C}} = 0.2, \sigma = 0.014$ or 0.14 or 1.4, $q = 0.91, b_0 = 0.04\ \mathrm{s}^{-1}, A^{\mathrm{eq}} = 5$, and a typical endosome radius of 1.2 μm. All concentrations are in fluorescence units per $\mu\mathrm{m}^2$ except A^{eq}, which is in fluorescence units per $\mu\mathrm{m}^3$. The inference errors are the median from five different Monte Carlo runs for five different data sets. The error bars are calculated by the bootstrap method. We simulated 12 bleached endosomes and 40 control endosomes, each with six fluorescence measurements spaced 30 s apart.

$br_{\mathrm{k}}^2/D_{\mathrm{A}}$ to be greater than unity and the recovery to be no longer reaction-limited.

We applied our method to investigate the interaction between β-arrestin and GPCRs (Fig. 1). β-arrestin binds to phosphorylated GPCRs and targets receptors for internalization. Three classes of GPCRs exist: class A receptors bind β-arrestin weakly. They recruit β-arrestin to the plasma membrane, but the receptor and β-arrestin complex dissociates at or near the plasma membrane (18). Class B receptors bind β-arrestin strongly and internalize with β-arrestin into endosomes (18). Class C receptors bind β-arrestin with an intermediate strength, but this binding is strong enough for β-arrestin to internalize with the receptors into endosomes (19). We consider the interaction of β-arrestin2 with two receptors: the bradykinin type 2

receptor (B2R), which is a class C receptor (19), and the angiotensin II receptor type 1A (AT1R), which is a class B receptor (18). Binding of β-arrestin2 to B2R is therefore expected to be weaker than its binding to AT1R.

Data for the recovery of the bradykinin receptor with β-arrestin2 and data from the corresponding control endosomes is shown in Fig. 2. The signal/noise ratio is $\sim$9. We find that C_0, the mean concentration of fluorescent complex at an endosome, is $\sim 8.3 \times 10^3$ fluorescence units per μm^2 and that σ, which determines the measurement error in the data, is $\sim 1.8 \times 10^4$ fluorescence units. Fig. 2 *B* shows the fluorescence concentration of the control endosomes: the fluorescence intensity of each endosome has been divided by the surface area of the endosome assuming that the endosome is spherical and using the microscope images to estimate its radius. Notice that there is still a significant spread in the initial fluorescence concentrations. We fit this spread, σ_C, to be $\sim 2 \times 10^3$ fluorescence units per μm^2. Unavoidable photobleaching from taking a confocal image causes the total fluorescence intensity of each control endosome to decrease on average. We find that the total intensity of an endosome decreases by a factor $q \simeq 0.92$ for each image.

Our FRAP results verify that B2R binds β-arrestin2 less strongly than AT1R: the half-life of the β-arrestin2 and B2R complex is $\sim$110 s, while the half-life of the β-arrestin2 and AT1R complex is $\sim$380 s, over three times longer (Fig. 4). These values correspond to an estimate of br_k^2/D_A of $\sim 10^{-4}$ implying that the recovery is reaction-limited and in the regime where our algorithm works best. Our fitted recovery curves are shown by the circles in Fig. 2. To further test our method, we consider the interaction of B2R with a truncated form of β-arrestin, which is missing its last 36 amino acids. This truncated β-arrestin has been shown to have stronger binding to agonist-occupied receptors (18,19,28). In agreement, we find that B2R forms a complex with the truncated form of β-arrestin2 with a lifetime of $\sim$320 s, almost three times longer than the lifetime of the complex of β-arrestin2 with B2R and similar to the lifetime of the β-arrestin2 and AT1R complex (Fig. 4).

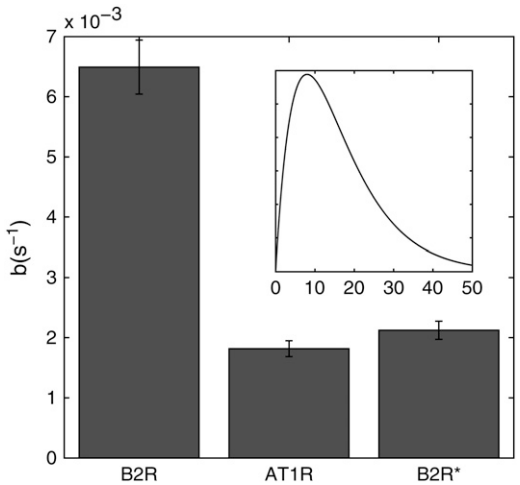

FIGURE 4 The inferred values of b for the bradykinin type-2 receptor with β-arrestin2 (B2R), the angiotensin II type 1A receptor with β-arrestin2 (AT1R), and the bradykinin type-2 receptor with truncated β-arrestin2 (B2R*). β-arrestin2 binding to the bradykinin receptor has a half-life of $\sim$2 min ($b = 0.0065 \pm 0.0004$ s^{-1}); β-arrestin2 binding to the angiotensin receptor has a half-life of $\sim$6 min ($b = 0.0018 \pm 0.0001$ s^{-1}); and truncated β-arrestin2 binding to the bradykinin receptor has a half-life of $\sim$5 min ($b = 0.0020 \pm 0.0002$ s^{-1}). The inferred values and errors in b are the mean and standard deviation of sampled b-values from a Monte Carlo run, averaged over five different runs. The inset shows the prior probability distribution for the diffusion coefficient of cytosolic β-arrestin2. It has a peak at $\sim 10\ \mu m^2$ s^{-1}.

DISCUSSION

Here we have developed a FRAP technique to infer the lifetime of protein complexes on intracellular vesicles (Fig. 1). We determine the lifetime at the endosome of complexes of β-arrestin with two G-protein-coupled receptors: the bradykinin type-2 receptor and the angiotensin II receptor type 1A. We use a Bayesian analysis that enables explicit incorporation of much of the variability seen from experiment to experiment. We allow variation in the concentration of receptors from endosome to endosome, measurement error, and photobleaching each time a confocal image is taken. In addition, we incorporate previous measurements of the diffusion coefficients of cytosolic protein to help estimate the diffusion coefficient of β-arrestin (Fig. 4, *inset*).

Our technique is quantitative and as such allows systematic investigation of the factors controlling the lifetimes of protein complexes. For example, we find that the β-arrestin complex with bradykinin receptor is much shorter-lived than the complex with angiotensin II receptor, as expected (18,19). This result helps confirm that the affinity of β-arrestin binding to the receptor controls the time taken for desensitization and receptor recycling (18).

Our analysis algorithm has a number of caveats. We assume that the bleached endosome is completely bleached. If this assumption is false, our estimate of b would be higher than the true value. We also assume sufficient quantities of cytosolic fluorescent arrestin to make the state of each endosome independent of each other. We ignore any unintentional bleaching of the cytosolic arrestin during the bleach, but such effects are probably small because the recovery is reaction-limited. To reduce the number of parameters controlling the recovery, we rescale the recovery equations (see Materials and Methods). This rescaling requires that the experimental measurements are taken at equal time intervals. Finally, we did not include any measurement error in the estimates of the radii of the endosomes taken from the confocal images. An additive normally distributed error could be easily included and would involve fitting the standard deviation of the distribution of this error and all the endosome radii in our Markov chain Monte Carlo scheme. In the reaction-limited regime,

the recovery of each endosome is independent of the radius of the endosome, and so we expect measurement errors of the radii to little affect our results.

With information on the number of receptors on the endosome, it would also be possible to infer the association rate for the β-arrestin and receptor interaction. Receptor numbers could be estimated by fluorescently tagging the receptors or perhaps by fluctuation techniques (29). Although our results indicate that the reaction between β-arrestin2 and GPCRs is reaction-limited, we can find a lower bound on the dissociation affinity by assuming that the association rate is diffusion-limited and so $\sim 10^9$ M^{-1} s^{-1} (30). We find a lower bound on the dissociation affinity for β-arrestin2 and B2R of $\sim 6 \times 10^{-12}$ M and for β-arrestin2 and AT1R of $\sim 2 \times 10^{-12}$ M.

Although we have demonstrated our FRAP technique on β-arrestin and G-protein-coupled receptors at endosomes, it should be applicable to any signaling protein at an intracellular vesicle interacting with a cytosolic partner. By providing accurate measurements of protein complex lifetimes, our method allows new quantitative investigations of cell biology and provides the in vivo parameters necessary for systems biology studies.

APPENDIX: MATHEMATICAL DERIVATIONS

Solving for the recovery curve

Eqs. 1, 2, and 6 can be simplified by rescaling. Letting

$$u = \frac{A - A_{eq}}{C_{eq}} r; \quad y = \frac{C - C_{eq}}{C_{eq}}; \quad r' = \frac{r}{r_k}$$
$$\tau = \frac{D_A t}{r_k^2}; \quad \tilde{f} = \frac{r_k f^*}{D_A}; \quad \tilde{b} = \frac{r_k^2 b}{D_A} \tag{21}$$

gives

$$\frac{dy}{d\tau} = \tilde{f} u\Big|_{r'=1} - \tilde{b} y; \quad y(0) = -1 \tag{22}$$

from Eq. 1 and

$$\frac{\partial u}{\partial \tau} = \frac{\partial^2 u}{\partial r'^2}; \quad \left[\frac{\partial u}{\partial r'} - u\right]_{r'=1} = \frac{dy}{d\tau}; \quad u(r, \tau = 0) = 0 \tag{23}$$

from Eqs. 2 and 6. The boundary condition Eq. 3 implies that u and $\partial u/\partial r$ must be finite as $r \to \infty$ because $\partial/\partial r\left(A/C_{eq}\right) = (\partial u/\partial r)(1/r) - u/r^2$. Equations 22 and 23 are a complete specification of the system. The recovery of the endosome as a function of time is given by $\rho(\tau) = 1 + y(\tau) = C(\tau)/C^{eq}$.

Equations 22 and 23 can be solved in Laplace space and the Laplace transform of $y(\tau)$ inverted numerically. Laplace-transforming with respect to τ and following standard methods (31), we find

$$\hat{y}(\tilde{s}) = -\left[\tilde{s} + \frac{\tilde{b}}{1 + \frac{\tilde{f}}{1 + \sqrt{\tilde{s}}}}\right]^{-1} \tag{24}$$

where $\hat{y}(\tilde{s})$ is the Laplace transform of $y(\tau)$. We numerically invert Eq. 24 with the MATLAB routine invlap.m (K. J. Hollenbeck, unpublished).

The reaction-limited solution

When diffusion is fast, binding of arrestin and the receptor become reaction-limited. The typical timescale of recovery is $1/b$, and Eq. 24 can be written as

$$\hat{y}(s) = -\frac{1}{b}\left[\frac{s}{b} + \left(1 + \frac{\tilde{f}}{1 + \sqrt{s/b} \cdot \sqrt{br_k^2/D_A}}\right)^{-1}\right]^{-1} \tag{25}$$

where we have removed the rescaling and s is in units of time. If $br_k^2/D_A \ll 1$, then

$$\hat{y}(s) \simeq \frac{-1}{s + \frac{b}{1 + \tilde{f}}} \tag{26}$$

which can be analytically inverted to give Eq. 7 with $b_{eff} = b/1+\tilde{f}$.

The diffusion-limited solution

If the reaction occurs quickly, $br_k^2/D_A \gg 1$, then the timescale of the recovery is r_k^2/D_A. Equation 24 can be written as

$$\hat{y}(s) = -\frac{r_k^2}{D_A}\left[\frac{sr_k^2}{D_A} + \frac{br_k^2}{D_a}\left(1 + \frac{r_k f^*/D_A}{1 + \sqrt{sr_k^2/D_A}}\right)^{-1}\right]^{-1}$$
$$\simeq -\left[s + \frac{bD_A}{f^* r_k}\left(1 + \sqrt{\frac{sr_k^2}{D_A}}\right)\right]^{-1} \tag{27}$$

when $br_k^2/D_A \gg 1$. The reaction is at quasi-equilibrium throughout the recovery, and the recovery curve is a function of only two parameters: the dissociation affinity, br_k/f^*, and D_A/r_k^2.

S.A.L. and P.S.S. both hold Tier II Canada Research Chairs. This work was supported by Canadian Institutes of Health Research grants (No. MOP-74603 and No. PRG-82673) to S.A.L, by a Natural Sciences and Engineering Research Council of Canada grant to P.S.S., and by the Mathematics of Information Technology and Complex Systems National Centre of Excellence.

REFERENCES

1. Reits, E. A., and J. J. Neefjes. 2001. From fixed to FRAP: measuring protein mobility and activity in living cells. *Nat. Cell Biol.* 3:E145–E147.
2. Phair, R. D., and T. Misteli. 2001. Kinetic modeling approaches to in vivo imaging. *Nat. Rev. Mol. Cell Biol.* 2:898–907.
3. Klonis, N., M. Rug, I. Harper, M. Wickham, A. Cowman, and L. Tilley. 2002. Fluorescence photobleaching analysis for the study of cellular dynamics. *Eur. Biophys. J.* 31:36–51.
4. Axelrod, D., D. E. Koppel, J. Schlessinger, E. Elson, and W. W. Webb. 1976. Mobility measurement by analysis of fluorescence photobleaching recovery kinetics. *Biophys. J.* 16:1055–1069.
5. Siggia, E. D., J. Lippincott-Schwartz, and S. Bekiranov. 2000. Diffusion in inhomogeneous media: theory and simulations applied to whole cell photobleach recovery. *Biophys. J.* 79:1761–1770.
6. Sbalzarini, I. F., A. Mezzacasa, A. Helenius, and P. Koumoutsakos. 2005. Effects of organelle shape on fluorescence recovery after photobleaching. *Biophys. J.* 89:1482–1492.
7. Sbalzarini, I. F., A. Hayer, A. Helenius, and P. Koumoutsakos. 2006. Simulations of (an)isotropic diffusion on curved biological surfaces. *Biophys. J.* 90:878–885.

8. Carrero, G., D. McDonald, E. Crawford, G. de Vries, and M. J. Hendzel. 2003. Using FRAP and mathematical modeling to determine the in vivo kinetics of nuclear proteins. *Methods*. 29:14–28.

9. Weiss, M. 2004. Challenges and artifacts in quantitative photobleaching experiments. *Traffic*. 5:662–671.

10. Sprague, B. L., and J. G. McNally. 2005. FRAP analysis of binding: proper and fitting. *Trends Cell Biol*. 15:84–91.

11. Kaufman, E. N., and R. K. Jain. 1990. Quantification of transport and binding parameters using fluorescence recovery after photobleaching. Potential for in vivo applications. *Biophys. J*. 58:873–885.

12. Carrero, G., E. Crawford, M. J. Hendzel, and G. de Vries. 2004. Characterizing fluorescence recovery curves for nuclear proteins undergoing binding events. *Bull. Math. Biol*. 66:1515–1545.

13. Sprague, B. L., R. L. Pego, D. A. Stavreva, and J. G. McNally. 2004. Analysis of binding reactions by fluorescence recovery after photobleaching. *Biophys. J*. 86:3473–3495.

14. Sprague, B. L., F. Muller, R. L. Pego, P. M. Bungay, D. A. Stavreva, and J. G. McNally. 2006. Analysis of binding at a single spatially localized cluster of binding sites by fluorescence recovery after photobleaching. *Biophys. J*. 91:1169–1191.

15. Pierce, K. L., R. T. Premont, and R. J. Lefkowitz. 2002. Seven-transmembrane receptors. *Nat. Rev. Mol. Cell Biol*. 3:639–650.

16. Claing, A., S. A. Laporte, M. G. Caron, and R. J. Lefkowitz. 2002. Endocytosis of G protein-coupled receptors: roles of G protein-coupled receptor kinases and β-arrestin proteins. *Prog. Neurobiol*. 66:61–79.

17. Moore, C. A., S. K. Milano, and J. L. Benovic. 2007. Regulation of receptor trafficking by GRKs and arrestins. *Annu. Rev. Physiol*. 69:451–482.

18. Oakley, R. H., S. A. Laporte, J. A. Holt, M. G. Caron, and L. S. Barak. 2000. Differential affinities of visual arrestin, β-arrestin1, and β-arrestin2 for G protein-coupled receptors delineate two major classes of receptors. *J. Biol. Chem*. 275:17201–17210.

19. Simaan, M., S. Bedard-Goulet, D. Fessart, J. P. Gratton, and S. A. Laporte. 2005. Dissociation of β-arrestin from internalized bradykinin B2 receptor is necessary for receptor recycling and resensitization. *Cell. Signal*. 17:1074–1083.

20. Kitano, H. 2002. Computational systems biology. *Nature*. 420:206–210.

21. Laporte, S. A., G. Servant, D. E. Richard, E. Escher, G. Guillemette, and R. Leduc. 1996. The tyrosine within the NPXnY motif of the human angiotensin II type 1 receptor is involved in mediating signal transduction but is not essential for internalization. *Mol. Pharmacol*. 49:89–95.

22. Berg, H. C., and E. M. Purcell. 1977. Physics of chemoreception. *Biophys. J*. 20:193–219.

23. Mackay, D. J. C. 2003. Information Theory, Inference, and Learning Algorithms. Cambridge University Press, New York, New York.

24. Metropolis, N., A. W. Rosenbluth, M. N. Rosenbluth, A. H. Teller, and E. Teller. 1953. Perspective on ''Equation of state calculations by fast computing machines''. *J. Chem. Phys*. 21:1087–1092.

25. Hastings, W. K. 1970. Monte Carlo sampling methods using Markov chains and their applications. *Biometrika*. 57:97–109.

26. Arrio-Dupont, M., G. Foucault, M. Vacher, P. F. Devaux, and S. Cribier. 2000. Translational diffusion of globular proteins in the cytoplasm of cultured muscle cells. *Biophys. J*. 78:901–907.

27. Wachsmuth, M., W. Waldeck, and J. Langowski. 2000. Anomalous diffusion of fluorescent probes inside living cell nuclei investigated by spatially-resolved fluorescence correlation spectroscopy. *J. Mol. Biol*. 298:677–689.

28. Kovoor, A., J. Celver, R. I. Abdryashitov, C. Chavkin, and V. V. Gurevich. 1999. Targeted construction of phosphorylation-independent β-arrestin mutants with constitutive activity in cells. *J. Biol. Chem*. 274:6831–6834.

29. Rosenfeld, N., T. J. Perkins, U. Alon, M. B. Elowitz, and P. S. Swain. 2006. A fluctuation method to quantify in vivo fluorescence data. *Biophys. J*. 91:759–766.

30. Lauffenburger, D. A., and J. Lindermann. 2003. Receptors: Models for Binding, Trafficking, and Signaling. Oxford University Press, New York, New York.

31. Carslaw, H. C., and J. C. Jaeger. 1986. Conduction of Heat in Solids. Oxford University Press, New York, New York.